A growing microcolony can survive and support persistent propagation of virulent phages

Rasmus Skytte Eriksen[a], Sine L. Svenningsen[b,1], Kim Sneppen[a], and Namiko Mitarai[a,1]

[a]Niels Bohr Institute, University of Copenhagen, DK-2100 Copenhagen, Denmark; and [b]Department of Biology, University of Copenhagen, DK-2200 Copenhagen, Denmark

Edited by Bruce R. Levin, Emory University, Atlanta, GA, and approved November 27, 2017 (received for review May 30, 2017)

Bacteria form colonies and secrete extracellular polymeric substances that surround the individual cells. These spatial structures are often associated with collaboration and quorum sensing between the bacteria. Here we investigate the mutual protection provided by spherical growth of a monoclonal colony during exposure to phages that proliferate on its surface. As a proof of concept we exposed growing colonies of *Escherichia coli* to a virulent mutant of phage P1. When the colony consists of less than ∼50,000 members it is eliminated, while larger initial colonies allow long-term survival of both phage-resistant mutants and, importantly, colonies of mostly phage-sensitive members. A mathematical model predicts that colonies formed solely by phage-sensitive bacteria can survive because the growth of bacteria throughout the colony exceeds the killing of bacteria on the surface and pinpoints how the critical colony size depends on key parameters in the phage infection cycle.

bacteria | spatial structure | coexistence | endemic | predator-prey

Virulent phages are ubiquitous, yet seemingly at odds with their own survival. As they kill their susceptible hosts, they suppress these to low population levels (1–3), creating a fragile and hugely competitive environment for themselves (4–6). By contrast, temperate phages have the option to lysogenize their host and thereby preserve their DNA through periods of low host availability (7, 8). This apparent advantage of temperate over virulent phages suggests the need for a more fine-grained understanding of virulence.

Notably, the virulent phage species present a quite diverse set of characteristics for their killing. Even under identical conditions, different species have average burst sizes that vary by more than a factor of 10 and have latency times that vary by a factor of 4 (9). Some virulent phages such as T3 and T7 are known to form particularly large plaques (10), while for example T4 forms rather small plaques due to lysis inhibition (10, 11), reflecting the variation in the "art of killing" (12).

Here we explore a demographic aspect of virulence, namely how a virulent phage propagates in a growing bacterial colony. Our investigation is inspired by visual inspection of the plaque formed by a virulent phage in Fig. 1. The picture shows a "clear" plaque, caused by one $P1_{vir}$ phage that was introduced onto a bacterial lawn consisting of *Escherichia coli* cells. A nearly clear region surrounds the initial infection at the center, but one can also observe increasingly larger faint colonies as one moves away from this center. Outside the plaque, the agar contains a dense collection of colonies that have grown to stationary phase without the influence of phages. Bacteria in the periphery of the plaque encountered phages relatively later, after each bacterial cell had grown to form a microcolony (13). The origin of the faint colonies at the plaque periphery has not been fully understood (14).

This paper explores the fate of growing bacterial colonies that are exposed to phages at various time points during their growth. A previously proposed scenario (14) discussed that cells in the center of a large microcolony may enter stationary phase and become unable to support the production of progeny phages. Although such a protection mechanism is certainly expected, recent work showed that the growth of even quite large *E. coli* colonies ($\sim 10^7$ cells) mimics the normal exponential growth of individual *E. coli* cells in liquid medium (15). This finding indicates that nutrients diffuse extensively through the colony. By contrast, phages may well adsorb in large numbers to susceptible cells on the colony surface and therefore only rarely reach deeper layers of the colony. Thus, we hypothesize that the continued growth from the inside of a sufficiently large colony could overwhelm killing on the colony surface. In combination with the phage-refractory state of stationary-phase cells, the result would be long-term survival of phage-sensitive cells inside the colony.

Here, we first construct a model of growing cells and infecting phages to numerically simulate the phage attack on a growing microcolony. The simulation suggests a sharp transition from elimination of the microcolony to its continued growth as the microcolony size at the time of the first phage encounter increases. We then show that the model prediction is consistent with an experiment by infecting *E. coli* colonies of different sizes with $P1_{vir}$ and monitoring their fate. Our study demonstrates that a sufficiently large colony indeed provides a refuge against $P1_{vir}$. The refuge counteracts the phages' ability to control bacterial biomass (6) and thereby allows the bacteria to circumvent the famous kill-the-winner (16) feature of phage predation in well-mixed environments.

Results

Model. We simulate microcolony growth by modeling each cell as a sphere, and each cell grows and divides exponentially with a minimum doubling time of ∼20 min. The repulsive force

Significance

Bacteria are repeatedly exposed to an excess of phages and carry evidence of this in terms of multiple defense mechanisms encoded in their genome. In addition to molecular mechanisms, bacteria may exploit the defense of spatial refuges. Here we demonstrate how bacteria can limit the impact of a virulent phage attack by growing as a colony which exposes only its surface to phages. We identify a critical size of the initial colony, below which the phages entirely eliminate the colony and above which the colony continues to grow despite the presence of phages. Our study suggests that coexistence of phages and bacteria is strongly influenced by the spatial composition of microcolonies of susceptible bacteria.

Author contributions: R.S.E., S.L.S., K.S., and N.M. designed research, performed research, analyzed data, and wrote the paper.

The authors declare no conflict of interest.

This article is a PNAS Direct Submission.

[1]To whom correspondence may be addressed. Email: mitarai@nbi.ku.dk or sls@bio.ku.dk.

This article contains supporting information online at www.pnas.org/lookup/suppl/doi:10.1073/pnas.1708954115/-/DCSupplemental.

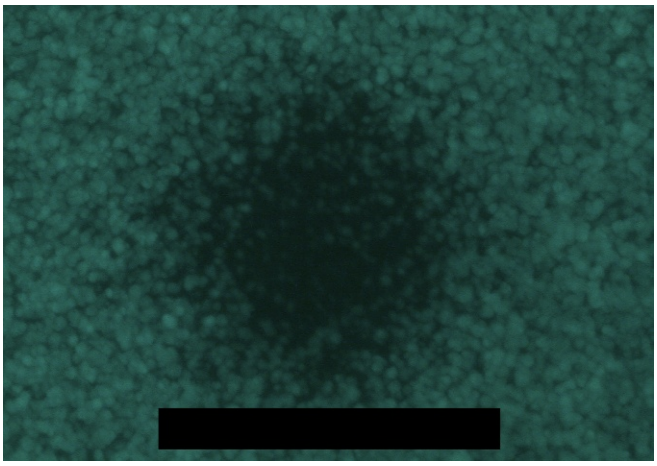

Fig. 1. Plaque formed by $P1_{vir}$. Green spheres are microcolonies of *E. coli* expressing green fluorescent protein. Note the faint colonies, which are seen across the plaque although less in its central region. (Scale bar: 300 μm.)

between the cells provides an overall spherical growth of the microcolony consisting of densely packed bacteria. At a certain time, we let the surface of a grown microcolony be surrounded by ∼2,700 phages and observe whether the phages kill all the cells or whether the cells can outgrow the ongoing lysis by the phages. The simulated microcolonies are rather small, and the explicit modeling of nutrient gradients inside a microcolony gave only minor growth rate differences across the colony (*SI Appendix*, section 3). Therefore, we here present the results from simulations that assume a constant nutrient level across the microcolony. The detailed simulation protocol is described in *Methods* and *SI Appendix*, section 1, with the default parameter values with dimensions (mostly measured in liquid culture conditions) in Table S1.

Fig. 2 illustrates model simulations with uninfected bacterial cells shown as blue spheres. Bacteria infected by phages are colored from yellow to red, where the ones closest to lysis are assigned the most reddish color. Each lysis event is modeled by replacement of the bacterium with 400 point-like phage particles at the end of the latency period. The progeny phages (not shown in the image) are allowed to diffuse and infect other bacteria. In this simulation, we assume that a phage particle adsorbs to a cell as soon as they overlap, mimicking the diffusion-limited scenario of adsorption. The phages adsorb equally well to uninfected cells and those that are already infected by another phage(s). We later study the effect of a smaller adsorption rate on microcolony growth.

In Fig. 2, *Upper* row, the first attack occurs at 3.25 h of growth, when the colony has a size of ∼220 members. Fig. 2, *Lower* row depicts a phage attack at 3.75 h where the colony size has reached ∼500 members. The smaller colony is eventually entirely eliminated, which would leave the fate of the phage particles to the chance that they reach another colony before they decay. In contrast, when the phages attack the larger colony, it survives and grows with phages persisting on the infected surface. The simulation showed that the distance phages can penetrate into the microcolony, ΔR, is roughly constant over time when the microcolony size is above the threshold of killing (*SI Appendix*, section 4). For the parameters used in Fig. 2, phages can infect about two layers of cells. This limited penetration is observed because new phages released by lysed cells on the surface mostly adsorb to the cells in their immediate vicinity instead of diffusing deeper into the microcolony. The result is a high multiplicity of infection of the surface cells (cf. ref. 17) with the cells closer to bursting located nearer to the surface (Fig. 2) and preservation of uninfected cells closer to the center.

Fig. 3 examines the predictions of the model. Fig. 3*A* shows the final growth rate of a colony as a function of the time at which it first encountered the phages. Indeed, the model predicts a sharp transition from extinction to persistent growth, when the size of the microcolony has surpassed a lower critical threshold. It is also apparent that if the first infection occurs sufficiently late to allow colony survival, the colony will reach a size where the growth penalty associated with infections at its surface becomes relatively small. Note that the growth rate is measured while the nutrient depletion is assumed to be negligible. In reality this assumption will ultimately break down when the inner part of the colony becomes increasingly shielded from available nutrients. The lack of nutrients will, however, also prevent or at least reduce phage proliferation (10, 14). Thus, if the colony is above the survival threshold, it is predicted to eventually maintain a large number of living sensitive cells in the center.

Assuming a constant penetration depth ΔR of the phages into a growing colony allows us to understand the steep size-dependent transition in microcolony fate. Suppose that a spherical microcolony of radius $R(t)$ at time t consists of an inner core of exponentially growing uninfected cells with growth rate of biomass g and an infected surface layer of a constant thickness ΔR. We further assume that infected cells will burst with a rate $1/\tau_L$, with τ_L being the latency time of the phage burst. This leads to the equation for the total volume $V(t) = \frac{4\pi}{3} R(t)^3$ to be

$$\frac{dV(t)}{dt} = \frac{4}{3}\pi \left[g(R(t) - \Delta R)^3 - \frac{1}{\tau_L} \left[R(t)^3 - (R(t) - \Delta R)^3 \right] \right],$$

where the first term in the brackets depicts the growth of the uninfected cells in the inner core, while the second term describes the lysis of the outer infected layer. Clearly, the growth of the total volume $dV(t)/dt > 0$ requires large enough $R(t)$ compared with ΔR. The critical threshold R_c for the initial size $R(0)$ is determined by $dV(0)/dt = 0$. The solution is given in *SI Appendix*, Eq. **S7** and fits well with the simulation (Fig. 3*B*). If we approximate the solution for a small penetration depth case ($\Delta R \ll R_c$), we get $R_c = 3[1 + (g\tau_L)^{-1}]\Delta R$ (derivation in *SI Appendix*, section 5), depicting that R_c increases with ΔR and that a smaller burst rate $1/\tau_L$ compared with the cell growth rate g decreases R_c.

R_c depends on the various parameters as demonstrated in Fig. 3 *B–D*. R_c grows roughly linearly with $1/\tau_L$ (Fig. 3*B*), because the latency time defines the timespan where an infected cell can

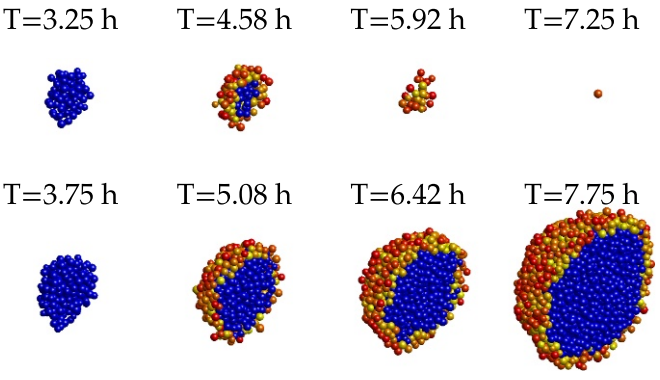

Fig. 2. Snapshots of simulations with half of the microcolonies presented. (*Upper* row) The case of a relatively early phage attack (infection at 3.25 h), which results in elimination of the microcolony. (*Lower* row) The history of a slightly later attack (infection at 3.75 h), which results in continued growth of the microcolony.

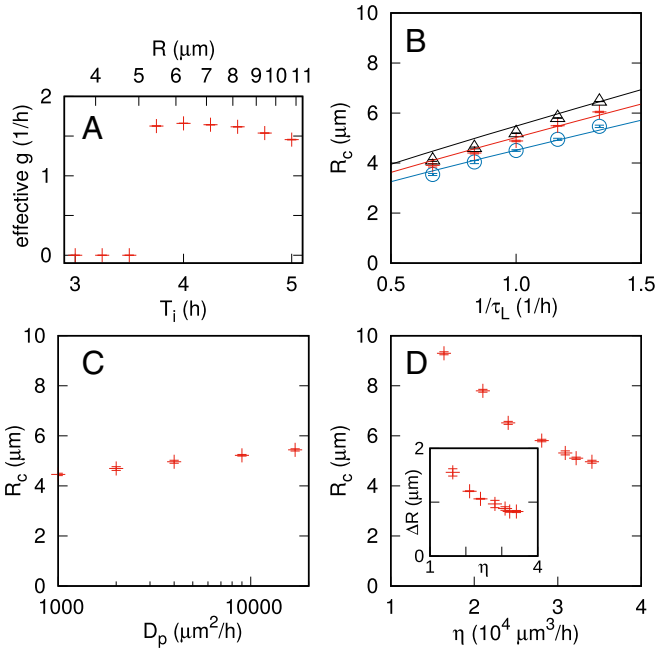

Fig. 3. Model predictions. (*A*) Long-term growth rate of phage-infected colony as a function of initial exposure time (T_i). The effective growth rate g was determined by fitting the analytical solution (*SI Appendix*, Eq. **S9**) of the linearized version of the model equation to the simulation time traces of the radius $R(t)$ (see *SI Appendix*, section 5 for details). The radius of the colony at the initial exposure time is shown on the top horizontal axis. (*B*) The critical radius R_c as a function of latency time τ_L for burst sizes of 100 (open blue circles), 400 (red crosses), and 1,000 (open black triangles). The fit of *SI Appendix*, Eq. **S7** to each data point is shown as a solid line, with the fitting parameter $\Delta R = 1.26$ μm, 1.40 μm, and 1.53 μm, respectively. (*C*) R_c as a function of the phage diffusion constant D_P. (*D*) R_c as a function of the phage adsorption rate η. *D*, *Inset* shows the phage penetration depth ΔR. The SEM is shown as error bars.

continue to shield the uninfected core by adsorbing additional phage particles until it undergoes lysis. The burst size affects ΔR and hence R_c, but changing the burst size from 100 to 1,000 increases the critical radius R_c only by about one cell layer with the given parameter set (Fig. 3*B*). A larger phage diffusion constant D_p only marginally increases the critical radius (Fig. 3*C*), because the phages are hindered from reaching the core cells by adsorption to the infected surface cells regardless of the magnitude of the diffusion constant.

Reducing the adsorption rate η from the diffusion-limited case causes a substantial increase in the critical radius R_c. To simulate small η we allowed the phage particles that overlap a cell to be repelled away and introduced a finite rate γ with which infection can occur while there is overlap. Reducing γ parameterizes a reduction of the phage adsorption rate η from the diffusion-limited value. The reduction of η dramatically increases the critical radius R_c (Fig. 3*D*). Note that the values of η shown are determined in the well-mixed condition (*SI Appendix*, section 2), and the actual adsorption events to densely packed hosts cannot be simply given by η multiplied by the densities of the phage and bacteria. The reduction of R_c is caused by an increased penetration depth ΔR as phages can diffuse deeper into the colony core before they adsorb to a cell, demonstrating the importance of the high multiplicity of infection of cells at the surface for the protection of the core.

Infection of *E. coli* Colonies with $P1_{vir}$. To test the above predictions in the laboratory, we performed infections of *E. coli* microcolonies with a virulent mutant of the phage P1, $P1_{vir}$ (18). This phage has a fairly long latency time of 60 min for *E. coli* growing in rich medium (9), thus facilitating a moderately small value of R_c. As the bacterial host, we used *E. coli* strain SP427 (19), which expresses green fluorescent protein (GFP) constitutively. The GFP expression allowed us to visualize the intact cells in the colonies using fluorescence microscopy. We grew the host cells embedded in a thin soft-agar layer on plates containing rich medium, which prevents the cells from swimming and causes them to form compact, approximately spherical colonies. We then sprayed phage lysate onto these plates at different times after incubation, thereby implementing phage attacks on colonies of different sizes (*Methods*). We sprayed enough phages that all of the phage-sensitive cells would have been killed if the same phage-to-cell ratio had been mixed in a homogeneous liquid culture (details in *SI Appendix*, section 9).

Fig. 4 shows images of representative colonies at the time of addition of phage $P1_{vir}$ and at 16 h of incubation after phage addition. Fig. 4, *Left* shows the dark-field images, whereas Fig. 4, *Right* shows the green fluorescence images, which visualize intact bacteria that contain GFP. The panel "5h" displays the rather small colony size that was typically obtained after 5 h of incubation. The "5h+16h" panel (Fig. 4, *Top*) shows the typical final colony after an additional 16 h of incubation without exposure to phage. In this case, the colony is not only large

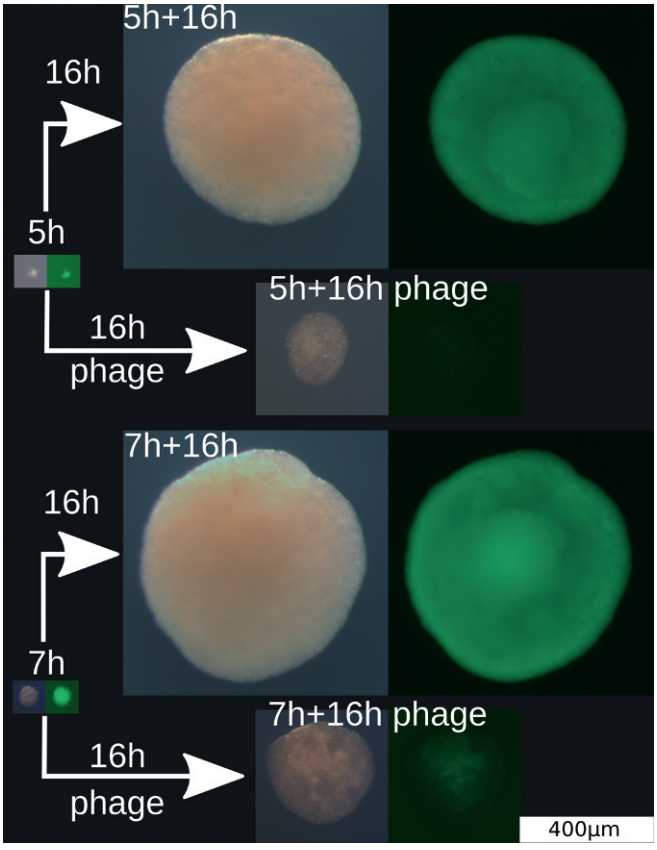

Fig. 4. Images of typical colonies before and after exposure to phages. The dark-field image and the corresponding green fluorescence image of the same colony are shown side by side. The green fluorescence images in the final colonies with phage exposure at 5 h and at 7 h spray time were collected at the same light source strength and with the same exposure time and are shown in the same magnification to allow direct comparison. Images of colonies that experienced different phage exposure times but identical total incubation times are shown in *SI Appendix*, Figs. S9 and S10.

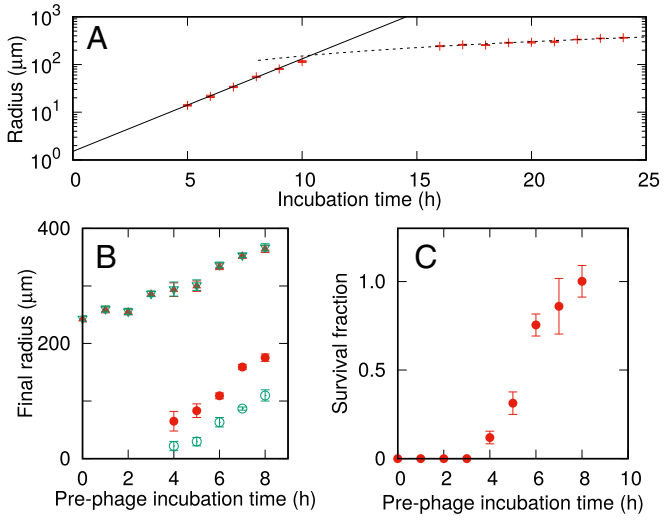

Fig. 5. $P1_{vir}$ infection of *E. coli* microcolonies. (*A*) Growth in colony radius over time in the absence of phages. The solid line marks an exponential fit with a doubling time of 31 min. The dashed line is a linear fit to growth in colony radius on longer timescales. The crossover point is ∼10 h. The radius was estimated from the colony image from the area A as $\sqrt{A/\pi}$. (*B*) Final colony size as a function of the incubation time before phage exposure. The solid red symbols show the estimates from dark-field images whereas the open green symbols show the radius estimated from the green fluorescence images. The triangles between 200 μm and 400 μm show the final radius of colonies in the absence of phages, while the circles show the final radius of colonies exposed to phages. The SEM is shown as error bars. (*C*) Number of visible colonies on plates sprayed with phages relative to the mean number of colonies on control plates without phages. The control plates had 76 ± 4 visible colonies per plate. The horizontal axis shows the microcolony growth time before the exposure to phages.

but also dense and homogeneously fluorescent. In contrast, the "5h+16h phage" panel (Fig. 4, *Upper Middle*) shows a typical final colony when the plate has been sprayed with phage lysate after 5 h of growth and then incubated 16 h after that. One sees that the colony has grown bigger after incubation in the presence of phages, but it exhibits only faint fluorescence, indicating that most of the colony shown in the dark-field image consisted of dead remnants of bacteria.

The typical colony obtained after 7 h undisturbed growth is shown in the "7h" panel in Fig. 4, *Bottom*, and is visibly larger than the typical colony after 5 h of incubation, reflecting the additional four doublings of biomass. The panel "7h+16h phage" shows the final size of this colony after it was exposed to phages and then incubated for 16 more hours. Although it is visibly smaller than the undisturbed colony in the "7h+16h" panel, one observes a fluorescent region in the middle, suggesting a substantial amount of surviving bacteria.

Using microscopy images, we measured the growth of colonies that had not been exposed to phages and show that the radius grows exponentially (Fig. 5*A*). This growth is consistent with a doubling time of 30 min for about 9 h until a size of 2×10^6 bacteria if we assume a spherical colony of dense cells with volumes of 1 μm^3. After about 10 h, the growth rate is reduced substantially and colony size eventually stabilizes at a level set by the initially available nutrients and the number of colonies per plate sharing those nutrients. Fig. 5*B* shows how this final colony size varies moderately between experiments without phage exposure (triangles). The final radius of 400 μm implies that our conditions allow colonies to reach $\sim 2 \times 10^8$ bacteria. Because slow-growing bacteria are smaller than rapidly growing bacteria (20), we cannot accurately deduce the actual number of bacteria in these colonies.

Predictably, exposure to phages alters the colonies dramatically. Fig. 5*B* (circles) shows the final size of colonies that were exposed to phages. In the dark-field recording we see a moderate change in the radius of final colonies from about 90 μm to about 180 μm as the phage exposure time is delayed. The corresponding change in size of the GFP-expressing part of the colony increases more dramatically from 20 μm to about 100 μm. In all cases, the outer layers of the colony appear dark, indicating that the surfaces of these colonies consist of bacterial debris from *E. coli* that were killed by phages. Fig. 5*C* quantifies the number of colonies per plate that are visible with the naked eye after the final incubation period for different prephage incubation times. The surviving fraction is normalized to the average number of visible colonies per control plate that were not exposed to phage. Almost no colonies had grown to visible size when the phages were introduced earlier than 4 h of incubation. The absence of surviving colonies was confirmed using fluorescence microscopy with 10× magnification. After this critical time, visible colonies emerged. When phages were introduced at 4 h, a few small colonies could be detected. When phages were introduced at 6 h and later, almost 100% of the initial cells grew to form visible colonies. Thus, this laboratory experiment reproduced a steep transition in the number of surviving colonies that depended on the size of the microcolony at the time of phage addition. Two additional repetitions of the experiment confirmed the jump in colony survival when phages were introduced after 5–6 h of prephage incubation (*SI Appendix*, section 6).

An alternative explanation for the microcolony size-dependent jump in colony survival (Fig. 5*C*) could be that the jump reflects the critical colony size at which there is a large probability that the colony contains one or more mutated cells that have become phage resistant at the time of phage exposure and therefore can continue to grow and form a colony despite the killing of all of the phage-sensitive cells. Phage resistance and our spatial refuge model are not mutually exclusive but could both contribute to colony survival. To estimate the frequency of resistant bacteria in the surviving microcolonies, we picked cells from 50 of the microcolonies exposed to phages and restreaked them onto fresh plates to obtain "offspring" colonies formed by individual surviving cells in the presence of the chelator sodium citrate, which inactivates free phages and thereby permits colony formation by both sensitive and resistant cells. Up to 10 randomly picked offspring colonies from each original microcolony were then tested for resistance to $P1_{vir}$ by cross-streaking (see *SI Appendix*, Table S2 for complete results).

Table 1, "offspring," shows that sensitive and resistant cells were found in approximately equal numbers among the randomly picked offspring colonies arising from microcolonies that had been sprayed with phage after 4–8 h of prephage incubation. While these numbers demonstrate the expected strong selection pressure favoring phage-resistant mutants, which increased in frequency from 1.2×10^{-5} in the starting culture to ∼0.5 in the surviving colonies, they also demonstrate that many phage-sensitive cells can survive the attack by $P1_{vir}$. Importantly, when the offspring are grouped by the microcolony they originated

Table 1. $P1_{vir}$ resistance test summary

Time, h	"Offspring"			Original microcolonies			
	Sensitive	Resistant	Total	All sensitive	Mix	All resistant	Total
4	47	13	60	4	1	1	6
5	22	10	32	4	0	1	5
6	20	50	70	2	0	5	7
7	41	45	86	4	1	4	9
8	51	49	100	5	1	4	10
Total	181	167	348	19	3	15	37

from (Table 1, original microcolonies), it is clear that no resistant cells were found in about half of the microcolonies from which we could recover live cells (19/37), suggesting that these colonies contained typically more than 90% phage-susceptible cells and therefore could not have survived due to protection by classical herd immunity. Furthermore, these susceptible colonies all grew substantially after exposure to phages, demonstrating that susceptible bacteria can dominate colony growth during prolonged phage exposure. We note that our inability to recover live cells from 13/50 of the sampled microcolonies does not mean that all cells in those colonies were dead, since we recovered cells from the soft-agar–embedded colonies by sampling them with a toothpick rather than extracting whole colonies.

Discussion

This paper argues for a type of herd immunity associated with consecutive layers of bacteria that shield each other from infection. The modeled colonies exposed to phages at various time points in their growth predicted the existence of a minimal critical size of microcolony above which the inner growth overwhelms the killing by phages on the colony surface. We experimentally demonstrated that shielding can take place, by showing that $P1_{vir}$-sensitive cells often constitute the majority of the survivors in growing $P1_{vir}$-infected colonies. Due to a strong selection pressure for $P1_{vir}$ resistance, at least in the outer layers of the microcolonies, phage-resistant mutants also accumulated in our experiments. The resistant mutants could protect phage-sensitive cells by herd immunity if they (*i*) interfere with the spread of phages and (*ii*) constitute a greater fraction of the microcolony than the herd immunity threshold (21). The $P1_{vir}$-resistant mutants we analyzed (*SI Appendix*, section 8) and the ones reported in the literature (22) all result in resistance because they abolish $P1_{vir}$ adsorption, meaning they are "invisible" to $P1_{vir}$ and do not interfere with the spread. Further, from half of the surviving colonies, 10 of 10 randomly picked offspring were all phage sensitive, certainly suggesting a below-threshold resistant fraction. Thus, while phage resistance predictably occurred in our experiments, it is unlikely to have played a significant role in the shielding of phage-sensitive cells in these microcolonies.

Experimentally, the critical microcolony growth time is not as sharp as in the numerical simulation. This is expected because the vertical position of the microcolonies varies within the ∼0.4-mm-thick top-agar layer, and the colonies at the bottom will be exposed to phages later than those nearer the top. We confirmed the jump of the survival fraction to almost 100% at around 6 h prephage incubation time in additional experiments where we varied the soft-agar thickness (*SI Appendix*, section 6). The additional time needed for diffusion through the top agar brings a conservative estimate of the actual critical phage arrival time to about 6–7 h, resulting in an estimated $R_c \approx 25\ \mu m$ critical microcolony radius. Image analysis confirmed that each final colony had grown significantly beyond this size, supporting the proposed survival scenario. Quantitatively, this R_c value is three to five times larger than the typical results of the simulation in Fig. 3. Part of this disagreement could be because we simplified the cell shape to be a sphere in the simulations, while *E. coli* is known to have an elongated rod shape. If the long edge of a cell is pointed vertically into the microcolony, as is apparently the norm for other rod-shaped bacteria (23), the burst of such a cell allows phages to penetrate significantly deeper than in our scenario. Thereby the elongated shape of *E. coli* increases the penetration depth ΔR and hence increases R_c proportionally.

The fate of a colony may not only depend on whether its growth can outrival the lysis on the surface. In particular, when bacteria grow slower, phage infections tend to yield smaller burst sizes with longer latency times (24, 25) and most phages cease propagation on stationary-phase cells (26). This means that a colony which approaches its resource-limited size may survive a phage attack simply because the phages cannot propagate. In our study, this effect was not important for the determination of the critical size, since the threshold for colony survival was at most 7 h, and exponential growth continued past the 9-h mark. Thus, the surviving colonies had certainly grown after encountering the phages.

Since our proposed mechanism does not rely on specific molecular components in either the host or the phage, we believe our findings will generalize to a broad range of bacterium–phage pairs, a prediction which should be experimentally tested. Our model further predicts that protection will be limited in special cases where the latency time is very short and/or the adsorption rate is small. A similar effect of adsorption rate was observed for λ phages infecting bacteria in biofilm (27), indicating the importance of optimization of adsorption rate for phages to spread in a spatially structured habitat. Finally, the survival of sensitive cells after overnight incubation in the presence of phages depends on the inability of phages to propagate on nongrowing cells. Therefore, we predict that phages which can continue killing of stationary-phase cells [e.g., T7 (14)] would not favor colony survival.

Theoretical models supplemented with experiments on phage–bacteria culture in liquid media demonstrated (1, 2, 16) that bacteria and virulent phages persistently can coexist. They do so in self-organized critical conditions where only one phage from each bacterial lysis event persists to infect another susceptible host. Our present study suggests to view this coexistence differently when dealing with bacteria growing in a gel or a semisolid, as for example in soil or even in submillimeter scale in ocean water (28). Because all new bacteria are generated from bacteria that are already present, the spatial distribution of the host will be maintained over long time periods. The destiny of released phages then becomes crucially dependent on the distances to new colonies of hosts, and the overall survival of a virulent phage may then rely on "farming" the local colony in a sustainable way.

The observation of bacterial colonies with an active core surrounded by an extended region of likely dead (nonfluorescent) bacteria suggests yet another possibility that may enhance colony robustness. As dead bacteria accumulate on the surface of the colony, phage particles may lose their DNA by injecting it into these hosts' remnants. Thus, the debris may cause a sink for phage DNA at the surface of the colony that further enhances survival in its core.

In any case, our paper suggests that the evolution of especially long latency time and high adsorption rate for a virulent phage may reflect its ability to live in a persistently infectious parasitic state on a growing bacterial colony. A related persistent infection pattern is seen in filamentous phages (e.g., M13) that, on the scale of the individual bacteria, maintains the host alive while producing phages (29). In contrast, phages with small adsorption rates and short latency times will more easily exterminate a colony. One outcome of our colony-focused "microcosmos" is thus that the "choice" of latency time for a phage is more than just an optimization between fast generations with few offspring and longer generations with much larger burst size (30). For lytic phages, the art of killing (12) has more facets than growth on a well-mixed host population.

Methods

Numerical Simulation. The motion of the cells and phage is modeled without inertia. The cells are modeled as 3D spheres that repel each other when they overlap (31). An uninfected cell grows exponentially with a nutrient-dependent rate and divides into two cells when it reaches a threshold volume. The median of the cell volume is set to be 1.3 μm^3. We assume nutrients are spatially homogeneous and consumed as the cells grow. A phage is modeled as a point particle that undergoes diffusion. When the phage

overlaps with a cell, a repulsive force is exerted from the cell. A phage overlapping with a cell is adsorbed with a rate γ. When a cell is infected by a phage, it produces phage particles after an average latency time τ_L (13). During the latency period, an infected cell can adsorb more phages. When a lysis occurs, β new phage particles are spawned uniformly around the cell's center and the cell is removed. The simulation starts with a single cell, which is allowed to establish a colony for the time duration T_i. At time T_i, phages are spawned uniformly in the simulated volume outside of the colony. Details are in *SI Appendix*, section 1. The code is available as Dataset S1.

Infection of *E. coli* Microcolonies with $P1_{vir}$. *E. coli* strain SP427 (19), an MC4100 derivative containing a chromosomally encoded $P_{A1/O4/O3}$::*gfp*mut3b gene cassette (32), was grown overnight in LB (33) supplemented with 50 μg/mL kanamycin. The culture was diluted to ∼400 cfu/mL in sterile MC buffer (50 mM $CaCl_2$, 25 mM $MgCl_2$) and kept at room temperature. Every hour, 250 μL of the diluted culture was mixed with 2.5 mL R-top agar (as in ref. 34 but with 5 g/L agar and 50 μg/mL kanamycin), plated on fresh R agar plates (as R top but with 12 g/L agar), and incubated at 37 °C to allow individual cells to form microcolonies. After a given incubation time at 37 °C, 0.5 mL of $P1_{vir}$ phage lysate (7×10^9 pfu/ml) was sprayed uniformly on the top agar surface, using a perfume bottle with an atomizer bulb (35), and the plate was incubated for another 16 h at 37 °C. One control plate without the addition of $P1_{vir}$ was processed along with triplicate phage-spray plates for each time point. The experiment was repeated three times with similar results. Details of the repeat experiments can be found in *SI Appendix*, section 6. Microscopy images were obtained using a Leica MZ16F fluorescence stereomicroscope and quantification was done by matlab code developed by the authors. The peripheral 1 cm of each plate was excluded in the analysis to avoid any effects of heterogeneity in phage spraying close to the edge. Six additional plates without phage addition were prepared as the control plates above and used for microscopy imaging to determine microcolony size from 5–10 h of incubation at 37 °C.

ACKNOWLEDGMENTS. The authors sincerely thank Stanley Brown for helpful discussions and Linda Hove Christensen for technical assistance. This work was funded by the Danish National Research Foundation (BASP: DNRF120) and the European Research Council under the European Union's Seventh Framework Programme (FP/2007 2013)/ERC Grant Agreement 740704.

1. Campbell A (1961) Conditions for the existence of bacteriophage. *Evolution* 15: 153–165.
2. Levin BR, Stewart FM, Chao L (1977) Resource-limited growth, competition, and predation: A model and experimental studies with bacteria and bacteriophage. *Am Nat* 111:3–24.
3. Lenski RE (1988) Dynamics of interactions between bacteria and virulent bacteriophage. *Adv Microb Ecol* 10:1–44.
4. Heilmann S, Sneppen K, Krishna S (2012) Coexistence of phage and bacteria on the boundary of self-organized refuges. *Proc Natl Acad Sci USA* 109:12828–12833.
5. Jover LF, Cortez MH, Weitz JS (2013) Mechanisms of multi-strain coexistence in host–phage systems with nested infection networks. *J Theor Biol* 332:65–77.
6. Haerter JO, Mitarai N, Sneppen K (2014) Phage and bacteria support mutual diversity in a narrowing staircase of coexistence. *ISME J* 8:2317–2326.
7. Stewart FM, Levin BR (1984) The population biology of bacterial viruses: Why be temperate. *Theor Popul Biol* 26:93–117.
8. Maslov S, Sneppen K (2015) Well-temperate phage: Optimal bet-hedging against local environmental collapses. *Sci Rep* 5:10523.
9. De Paepe M, Taddei F (2006) Viruses' life history: Towards a mechanistic basis of a trade-off between survival and reproduction among phages. *PloS Biol* 4:e193.
10. Demerec M, Fano U (1945) Bacteriophage-resistant mutants in *Escherichia coli*. *Genetics* 30:119–136.
11. Hershey AD (1946) Mutation of bacteriophage with respect to type of plaque. *Genetics* 31:620–640.
12. Tzu S(ca. 450 BC) *Sun Tzu on the Art of War: The Oldest Military Treatise in the World, Translated from the Chinese with Introduction and Critical Notes*, trans Giles L (1910) (Luzac & Company, London).
13. Mitarai N, Brown S, Sneppen K (2016) Population dynamics of phage and bacteria in spatially structured habitats using phage λ and *Escherichia coli*. *J Bacteriol* 198: 1783–1793.
14. Abedon S, Yin J (2008) Impact of spatial structure on phage population growth. *Bacteriophage Ecology*, ed Abedon S (Cambridge Univ Press, Cambridge, UK), Vol 15, pp 94–113.
15. Shao X, et al. (2017) Growth of bacteria in 3-d colonies. *PLoS Comput Biol* 13:e1005679.
16. Thingstad TF (2000) Elements of a theory for the mechanisms controlling abundance, diversity, and biogeochemical role of lytic bacterial viruses in aquatic systems. *Limnol Oceanogr* 45:1320–1328.
17. Taylor BP, Penington CJ, Weitz JS (2017) Emergence of increased frequency and severity of multiple infections by viruses due to spatial clustering of hosts. *Phys Biol* 13:066014.
18. Ikeda H, Tomizawa Ji (1965) Transducing fragments in generalized transduction by phage p1: I. Molecular origin of the fragments. *J Mol Biol* 14:85–109.
19. Bahl MI, Sorensen SJ, Hansen LH (2004) Quantification of plasmid loss in Escherichia coli cells by use of flow cytometry. *FEMS Microbiol Lett* 232:45–49.
20. Bremer H, Dennis PP (1996) Modulation of chemical composition and other parameters of the cell by growth rate. *Escherichia coli and Salmonella,* ed Neidhardt FC (ASM Press, Washington, DC), pp 1553–1569.
21. Payne P, Geyrhofer L, Barton NH, Bollback JP (2017) CRISPR-based herd immunity limits phage epidemics in bacterial populations. bioRxiv:10.1101/181487.
22. Franklin NC (1969) Mutation in *galu* gene of *E. coli* blocks phage p1 infection. *Virology* 38:189–191.
23. Drescher K, et al. (2016) Architectural transitions in *Vibrio cholerae* biofilms at single-cell resolution. *Proc Natl Acad Sci USA* 113:E2066–E2072.
24. Cohen SS (1949) Growth requirements of bacterial viruses. *Bacteriol Rev* 13: 1–24.
25. Weitz JS, Dushoff J (2008) Alternative stable states in host–phage dynamics. *Theor Ecol* 1:13–19.
26. Abedon ST, Yin J (2009) Bacteriophage plaques: Theory and analysis. *Bacteriophages: Methods and Protocols: Isolation, Characterization, and Interactions*, eds Clokie MRJ, Kropinski A (Humana Press, New York), Vol 1, pp 161–174.
27. Gallet R, Shao Y, Wang N (2009) High adsorption rate is detrimental to bacteriophage fitness in a biofilm-like environment. *BMC Evol Biol* 9:241.
28. Azam F, Malfatti F (2007) Microbial structuring of marine ecosystems. *Nat Rev Microbiol* 5:782–791.
29. Kehoe JW, Kay BK (2005) Filamentous phage display in the new millennium. *Chem Rev* 105:4056–4072.
30. Abedon ST, Herschler TD, Stopar D (2001) Bacteriophage latent-period evolution as a response to resource availability. *Appl Environ Microbiol* 67:4233–4241.
31. Mitarai N, Jensen MH, Semsey S (2015) Coupled positive and negative feedbacks produce diverse gene expression patterns in colonies. *mBio* 6:e00059-15.
32. Normander B, Christensen BB, Molin S, Kroer N (1998) Effect of bacterial distribution and activity on conjugal gene transfer on the phylloplane of the bush bean (*Phaseolus vulgaris*). *Appl Environ Microbiol* 64:1902–1909.
33. Bertani G (1951) Studies on lysogenesis. I. The mode of phage liberation by lysogenic *Escherichia coli*. *J Bacteriol* 62:293–300.
34. Miller JH (1972) *Experiments in Molecular Genetics* (Cold Spring Harbor Lab Press, Cold Spring Harbor, NY).
35. Schedl P, Primakoff P (1973) Mutants of *Escherichia coli* thermosensitive for the synthesis of transfer RNA. *Proc Natl Acad Sci USA* 70:2091–2095.

Supporting Information Appendix: A Growing Microcolony can Survive and Support Persistent Propagation of Virulent Phages

Rasmus Skytte Eriksen, Sine Lo Svenningsen, Kim Sneppen, Namiko Mitarai

November 13, 2017

Contents

1 Simulation method

1.1 Detailed protocol of the numerical simulation

Cell growth and cell-cell interaction

We constructed a 3-dimensional model of cells and surrounding phage particles. The cell are labeled by an index i and modeled as spheres with radius r_i, a position $\vec{x}_i$, and a state S_i. The cell experiences a repulsive potential V_{ij} from every other cell j of the form $V_{ij}(d_{ij}) = \frac{\tilde{k}}{2}\left(\frac{d_{ij}-r_i-r_j}{r_i+r_j}\right)^2$ if $d_{ij} \leq r_i + r_j$. The harmonic potential is chosen as it is the simplest repulsive potential and it has been used previously to model cell-cell interaction [1]. Here $\vec{d}_{ij} = \vec{x_i} - \vec{x_j}$ and $d_{ij} = ||\vec{d}_{ij}||$ is the euclidean distance between the cells. $\tilde{k}$ parametrizes the repulsion strength. The potential is set to be zero when $d_{ij} > r_i + r_j$. The motion of cells is computed in the over-damped limit ($m\ddot{x} \approx 0$), leading to the equation of motion: $\dot{\vec{x}}_i = -\frac{1}{\mu}\sum_{j\neq i}\frac{\mathrm{d}}{\mathrm{d}d_{ij}}V_{ij}\hat{\vec{d}}_{ij}$, where $\hat{\vec{d}}_{ij}$ is the unit vector parallel to $\vec{d}_{ij}$ and μ is a viscosity parameter. This viscosity and the repulsion strength $\tilde{k}$ can be absorbed together to a single variable k.

Cell growth follows a Monod growth, $\dot{r_i} = \frac{g(n)}{3}r_i$, where the nutrient-dependent growth rate $g(n) = g_{\max}\frac{n}{n+K}$. The maximal growth rate $g_{\max}$ is taken to be $\frac{1}{30\ \mathrm{min}}$ which corresponds to a doubling time of approximately 20 minutes. The Michelis-Menten constant was chosen to be $K = n(t=0)/5$.

Nutrient depletion

For simplicity, we only allow uninfected cells to grow and consume nutrients. We further assume that nutrients diffuse infinitely fast and are not hindered by the presence of the cells. Hence there is no spatial dependency in the growth rate. We confirmed that the relevant range of colony sizes was small enough that the simulation with a finite diffusion rate of nutrient with realistic parameters did not deviate noticeably from our infinite diffusion simulation. The depletion of nutrients takes the form $\dot{n} = -\frac{g(n)}{V}\sum_i \delta_{S_i,0}$, where state variable $S_i = 0$ denotes that the cell i is uninfected by phage, δ is the Kronecker delta function, and V is the volume of the system.

Cell Division

Each cell grows until it reaches the volume 2 $\mu\mathrm{m}^3$ (or $R_d = 0.782$ μm) where it divides. The choice for R_d is such that the median cell volume in the simulation is 1.3 $\mu\mathrm{m}^3$. During division, the parent cell p is removed and two daughter cells are placed close to the center of the parent cell with some randomness $x_i^{(j)} = x_p^{(j)} + \zeta$, where $i = (1,2)$ refer to the daughter cells, (j) denotes the j'th component of the position $\vec{x}$ and ζ is a uniformly distributed number in $[-\frac{R_d}{4}, \frac{R_d}{4}]$. One daughter cell receives the fraction $\alpha \sim 0.5$ of the parents volume, while the other receives the remaining fraction: $r_1 = r_p\alpha^{\frac{1}{3}}$ and $r_2 = r_p(1-\alpha)^{\frac{1}{3}}$. Here noise is introduced through the random number α that is drawn from the Normal distribution with average 0.5 and standard deviation 0.1. Noise in the cell position and the cell size is introduced to avoid complete synchronization of the cell divisions as well as an artificially regular packing of the cells [2].

Phages

The phages are treated as individual point particles described with positions $\vec{y}$. The phages diffuse in the simulation volume, following the over-damped Langevin equation: $\dot{y}_k^{(j)} = \vec{F}_k(y_k^{(j)}(t)) + \xi(t)$, where $y_k^{(j)}$ is the jth-component of the position of the k'th phage; $\xi(t)$ is a noise term with a Gaussian probability distribution: $\langle\xi(t)\rangle = 0$ and $\langle\xi(t),\xi(t')\rangle = 2D_p\delta(t-t')$. There is no phage-phage interaction and when there is no cell-phage collisions the force term vanishes $\vec{F}_k = 0$. However, when a phage collides with a cell it is exposed to a repulsive force described by the interaction potential $V_k(d_{ki}) = \frac{\tilde{k}}{2}\left(\frac{d_{ki}-r_i}{r_i}\right)^2$ if $d_{ki} \leq r_i$, where d_{ki} is the euclidean distance between the k'th phage and the i'th cell with radius r_i. Furthermore, we include phage decay at a rate δ. The simulation was done in a cube of volume V with a reflective boundary conditions for the phages.

Cell-Phage interaction

Collision between phage k and cell i is defined as $d_{ki} \leq r_i$. The infection of the i'th cell by the k'th phage occur at a rate γ as long as the phage is within the cell radius. When the cell is infected by the phage, the state S_i is set to $S_i = 1$ if the cell was previously in the uninfected state ($S_i = 0$), otherwise the state is unchanged. To take into account the time delay before cell lysis, we use a ten-step Poisson process [3]. It starts when a cell is first infected and we increase the cell state S_i at a rate $10/\tau_L$ until the state is $S_i = 11$, where lysis occurs and β new phages are spawned uniformly around the cell's center and the cell is removed. We assume τ_L is inversely

proportional to the host growth rate $g(n)$ as $\tau_L = 1/(rg(n))$ to reflect the phage reproduction dependence on the host metabolism [3].

$\gamma = \infty$ describes the diffusion limited adsorption of phage. The phage adsorption rate η in Fig. 3D in main text was adjusted by changing γ, where η for a given γ was measured by simulating adsorption to a single cell in a limited volume.

Simulation initialization

The simulation starts with a single cell of volume 1.3 μm^3, which is allowed to establish a colony for T_i time, after which the phages are added. At time T_i, the geometric center of the colony is computed $x_{gc}^{(j)} = \frac{1}{N}\sum_i x_i^{(j)}$, where N is the number of cells at time T_i. The maximal distance of any cell to the geometric center $r_{\max} = \max_i ||\vec{x_i} - \vec{x_{gc}}||$ is computed. Then $P_0 \cdot V$ phages are spawned uniformly in the simulation space outside the sphere defined by position $\vec{x_{gc}}$ and radius $r_{\max}$.

Time Integration

For the presented data here, the model was implemented using the explicit Euler method with a time-step of $\Delta t = 10^{-6}$. The consistency of the integration method were confirmed by checking the results are the same with different time-step and with different integration methods (the standard fourth-order Runge-Kutta method and the fifth order Runge-Kutta-Dormand-Prince method were tested for solving the deterministic part of the equations) at a few selected parameter sets.

1.2 Simulation parameters

Table S1: Summary of the default parameters. These values are used unless otherwise mentioned. The values are chosen to be applicable for phage P1 parameters when available.

Name	Value	Units	Description	Comments / References
ΔT	10^{-6}	h	Size of the time step	
L_{box}	65	μm	Side length of simulation volume	
n_0	0.5	$1/\mu$m^3	Initial concentration of nutrient	
g_{max}	2	1/h	Maximal growth rate for the cells	Based on liquid culture conditions / [3]
K	$n_0/5$	$1/\mu$m^3	Michaels-Menten constant for Monod growth	Based on liquid culture conditions / [3]
R_d	0.782	μm	The length scale for division	
k	10^3	μm^2/h	Parameter for cell-cell interaction potential	
P_0	0.01	$1/\mu$m^3	Density of invading phage	
γ	∞ [1]	1/h	Phage infection rate for diffusion limited case	
	10^5 to 10^6	1/h	to reduce the phage adsorption rate	
β	400		Burst size	Based on liquid culture conditions / [4]
δ	0.003	1/h	Rate of phage decay	Based on liquid culture conditions / [4]
r	0.6		Constant for lysis latency time	Based on liquid culture conditions / [4]
D_P	$4 \cdot 10^3$	μm^2/h	Diffusion constant for the phage	1/10 of λ phage diffusion constant, estimate based on the small plaque size /[3]
D_n	$4 \cdot 10^5$	μm^2/h	Diffusion constant for the nutrient	Based on liquid culture conditions / [3] Used in supplement

1.3 Outline of simulation implementation

The algorithm of the simulation is shown as a pseudo-code in Algorithm 1 and goes as follows:

1. Phages infect bacteria
2. Infection stage is updated, and cells marked for bursting
3. Movement is calculated for phages and cells (but not executed)
4. Nutrients are consumed and cells are grown
5. The movement is executed, and phages decay, and cells burst

Algorithm 1 The update step

for all p_i **do** ▷ Loop over all phages in the system
  if PhageInfection(p_i) == 1 **then** ▷ PhageInfection returns 1 if phage successfully infected a cell
    p_i is deleted.
  end if
end for
for all c_i **do** ▷ Loop over all cells in the system
  GrowInfection(c_i) ▷ GrowInfection drives the infections forward if cell is infected
end for
for all c_i **do** ▷ Loop over all cells in the system
  CellMovement(c_i) ▷ Compute the movement of the cell
end for
for all p_i **do** ▷ Loop over all cells in the system
  PhageMovement(p_i) ▷ Compute the movement of the phage
end for
$n \leftarrow n - \frac{1}{V} g_{max} \cdot \frac{n}{n+K} \cdot \sum_{c_i} \delta_{S_i,0} \cdot \Delta T$ ▷ Consume nutrient
for all c_i **do** ▷ Loop over all cells in the system
  if $S_i == 0$ **then** ▷ Check if cell is uninfected
    GrowCell(c_i) ▷ Grow the cell and divide if radius increases above threshold
  end if
end for
for all c_i **do** ▷ Loop over all cells in the system
  if $S_i == 11$ **then** ▷ Check if cell is lysed
    c_i is deleted.
  else
    ApplyMovement(c_i) ▷ Execute the movement of the cells
  end if
end for
for all p_i **do** ▷ Loop over all phages in the system
  if $rand() \leq \delta \cdot \Delta T$ **then** ▷ Check if phage decays
    p_i is deleted.
  else
    ApplyMovement(p_i) ▷ Execute the movement of the phages
  end if
end for

2 Determining the adsorption rate

We determine the adsorption rate η as a function of the infection rate γ, by considering the free space diffusion of phages. This is achieved by using our simulation framework to measure the time it takes for a phage to hit and successfully adsorb to a small target. We construct a small spherical target of radius $R = 0.677\mu$m (median cell volume) inside a box of size $L^3_{box} = 30 \times 30 \times 30\mu m^3$. We then simulate the adsorption of 10000 phage particles, and measure the distribution of free phages as a function of time for every value of γ used in the article. Snapshots of the free phage distribution are shown in Fig. S1 for $\gamma = 10^6$ h^{-1}.

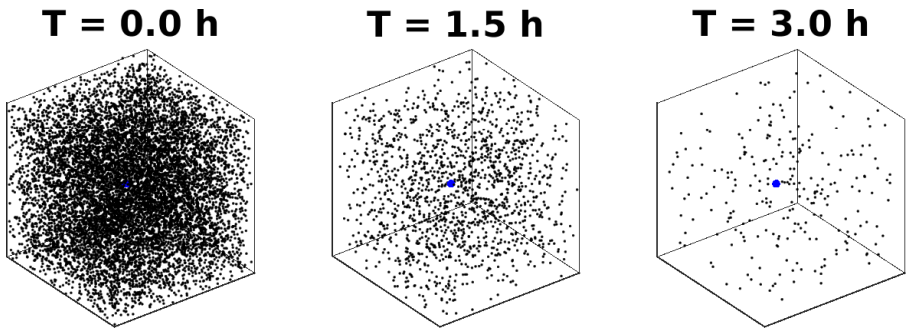

Figure S1: Snapshots of the adsorption simulation for $\gamma = 10^6$ h^{-1} at times $T = 0$ h, $T = 1.5$ h and $T = 3.0$ h. Each black dot represents a phage and the blue sphere represents the phage target.

The distribution of the number of free phages can be measured against T/L^3_{box} (blue points in Fig. S2 (left)). From this distribution, the adsorption coefficient can be estimated by fitting an exponential $A\exp(-\eta T/L^3_{box})$ to the blue points. The fitting parameter η (μ m^3/h) gives the adsorption rate in a well-mixed liquid condition, where the overall infection rate per unit volume would be given by η multiplied by densities of bacteria and phages.

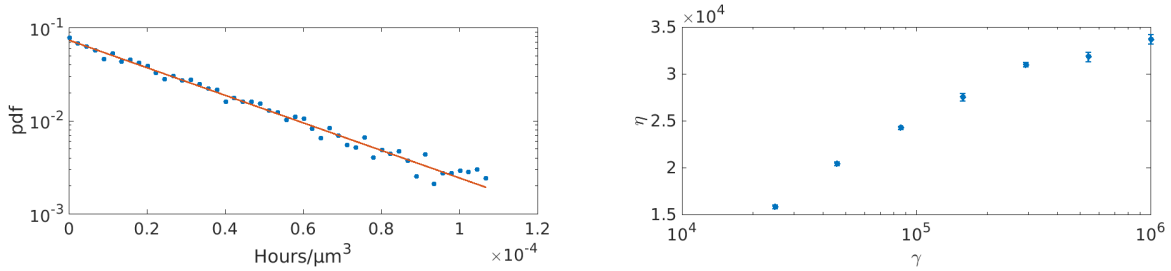

Figure S2: **Left:** The distribution of free phages as a function of T/L^3_{box} (blue points) and fit of $A\exp(-\eta T/L^3_{box})$ (red line). The corresponding adsorption coefficient is $\eta = (3.41 \pm 0.7)\mu m^3/h$. **Right:** The fit-values of η as a function of γ.

This process is repeated for every value of γ, which allows us to map the relationship between the parameters γ and η. The realized relation is shown in Fig. S2 (right).

3 Comparison with explicit modeling of nutrient diffusion and local consumption in microcolony growth

We investigate the accuracy of using the meanfield approximation for nutrient depletion:

$$\dot{n} = -\frac{g(n)}{V}\sum_i \delta_{S_i,0}, \tag{S1}$$

and compare it to the complete field computation. For the complete field computation, we construct a cubic grid for the space: $x_i = i\Delta_{\text{grid}}$, $y_j = j\Delta_{\text{grid}}$ and $z_k = k\Delta_{\text{grid}}$, and divide the time into the discrete points: $t_l = l\Delta T$. For this grid, we define the density of susceptible cells $S(i,j,k,t_l)$, by assigning each cell to the closest grid point. The complete field computation has the continuous form:

$$\dot{n} = -g(n(\vec{x},t)) \cdot S(\vec{x},t) + D_n\nabla^2 n(\vec{x},t). \tag{S2}$$

In our discretized scheme the field equation becomes:

$$\frac{n^{l+1}_{i,j,k} - n^{l}_{i,j,k}}{\Delta T} = -g(n^{l}_{i,j,k}) \cdot S^{l}_{i,j,k} + D_n \hat{\vec{L}} n^{l}_{i,j,k}, \tag{S3}$$

Where the Laplace-operator $\hat{\vec{L}}$ computes the diffusion on the grid. Using the central difference the explicit computation becomes:

$$D_n \hat{\vec{L}} n^{l}_{i,j,k} = \frac{D_n}{\Delta^2_{\text{grid}}}(n^{l}_{i-1,j,k} + n^{l}_{i+1,j,k} + n^{l}_{i,j-1,k} + n^{l}_{i,j+1,k} + n^{l}_{i,j,k-1} + n^{l}_{i,j,k+1} - 6n^{l}_{i,j,k}). \tag{S4}$$

We test the difference between the full field computation and the meanfield computation using the parameters listed in table S1 with two exceptions: $L_{\text{box}} = 50$ μm and $n_0 = 0.1$ μm^{-3}. We observe only minute differences

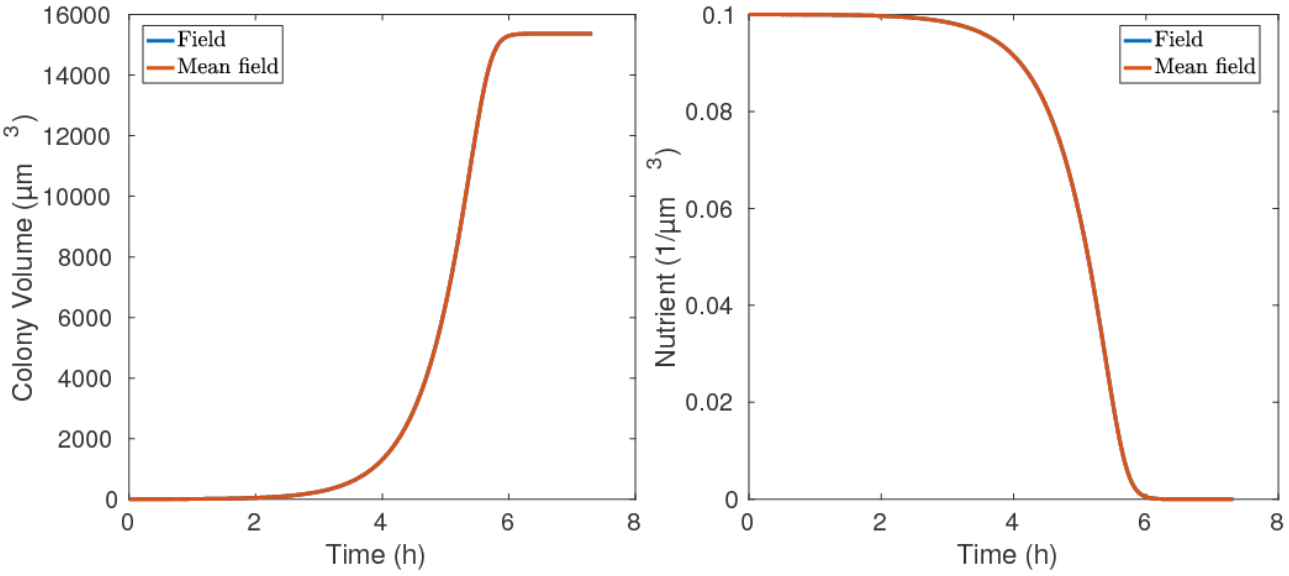

Figure S3: Difference between the full field computation (blue) and the meanfield approximation (red). Because the two curves overlap, the blue curve cannot be visualized in the figure. **Left**. The volume of the colony as a function of time. **Right**. The density of nutrients in the simulation.

between the methods on this scale, but we expect the impact to increase as the total colony volume increases.

4 Measuring the penetration depth from simulations

From the simulations, we observe that the phages can only penetrate the bacterial colony up to a certain depth. This happens because the phages tend to adsorb to the cells close to the surface, which are typically already infected by other phages and get super-infected while they are undergoing latency time before the next phage burst. As a result, the system self-organize to have the cells close to the burst at the surface and the cells in early stage of infection closer towards the core, as seen in Fig. 2 in the main text. By developing a metric to measure this penetration depth, we can observe how the phage parameters influence the phages' ability to invade the colony.

We have operationally measured this penetration depth by first determining the geometric center of the colony $\vec{x}_{gc}(t) = \frac{1}{N}\sum_{i=1}^{N} \vec{x_i}(t)$, where N is the total number of cells in the colony. Next we measure the distance $d_{i,gc}(t)$ from every infected cell to the geometric center as $d_{i,gc}(t) = \|\vec{x}_i(t) - \vec{x}_{gc}(t)\|$. The penetration depth $\Delta R(t)$ is then taken as twice the standard deviation of the distribution of $d_{i,gc}(t)$ at time t.

In Fig. S4, we show a typical example of the penetration depth as a function of time. We notice that the penetration depth initially increases but after approximately 2 hours it stops increasing and reaches a steady state.

In order to plot ΔR for each parameter set in Fig. 3D inset, we converted these time-series into a single measure by cropping the first two hours of each time-series, and taking the mean and standard deviation of the remaining data as the penetration depth and uncertainty, respectively. Since we took an ensemble average of three runs for every parameter set, we took the weighted average over the ensemble and use the standard error of the mean as the error bar in the plot.

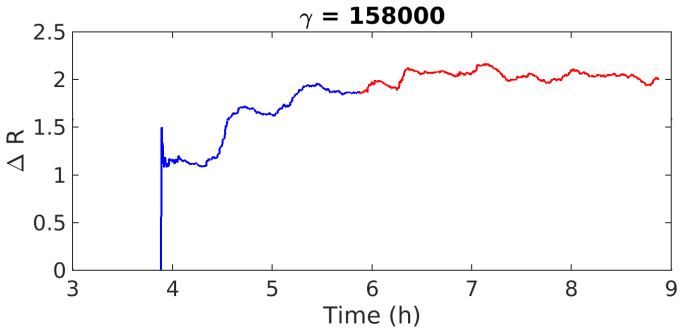

Figure S4: Example of the penetration depth as a function of time. The red section indicates the data used for the steady state measurement. See text for details.

5 Modeling colony growth under phage attack

5.1 Model equation and solution

We model the bacterial microcolony as a solid sphere consisting of an inner core of susceptible cells and a thick outer shell of depth ΔR of infected cells. The model system is illustrated in Fig. S5.

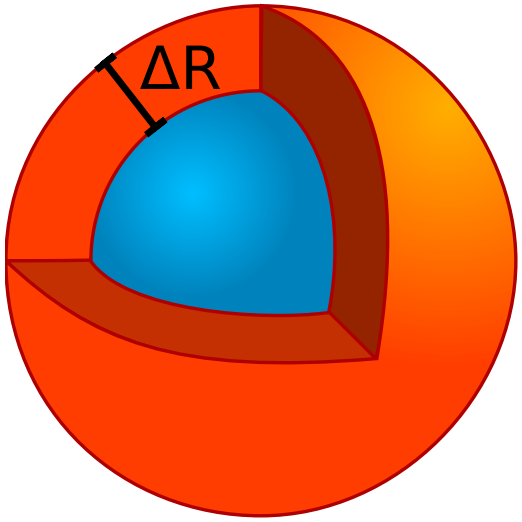

Figure S5: The model system: The cell colony is considered a solid sphere, where the susceptible cells are located in the core (blue), and the infected cells are located as a thick shell (orange) of depth ΔR around the core.

The dynamics of the microcolony can be described by the volume of the core V_O and of the shell $V_{\Delta R}$.

$$\frac{\mathrm{d}V}{\mathrm{d}t} = \frac{\mathrm{d}V_O}{\mathrm{d}t} + \frac{\mathrm{d}V_{\Delta R}}{\mathrm{d}t}$$

The cells are assumed to be in the exponential growth phase and thus the core of uninfected bacteria grows at a rate g and the infected shell is diminished at a rate $rg = 1/\tau_L$ with τ_L being the latency time of phage burst.

$$\frac{\mathrm{d}V}{\mathrm{d}t} = gV_O - rgV_{\Delta R}$$

This expression can be rewritten in terms of the colony radius R.

$$\frac{\mathrm{d}R}{\mathrm{d}t} = \frac{g}{3}\left[(r+1)\frac{(R-\Delta R)^3}{R^2} - rR\right] \tag{S5}$$

This equation allows for stable solutions as long as the growth term is larger than the decay term. There is as such a critical radius R_C, where the derivative is zero:

$$(r+1)(R_C - \Delta R)^3 - rR_C^3 = 0 \tag{S6}$$

The solution of this equation linearized with ΔR is presented in the main text eq. (2). The full solution of eq. (S6) is given by:

$$R_C = \Delta R \left(r^{\frac{1}{3}} (r+1)^{\frac{2}{3}} + r^{\frac{2}{3}} (r+1)^{\frac{1}{3}} + r + 1 \right). \tag{S7}$$

Other than predicting the threshold value of the colony size, (S5) can also be solved by using a few approximations, and then be compared to the volumetric growth curves of the colonies. We expand the first term in eq. (S5) in terms of $\Delta R/R$:

$$\frac{(R-\Delta R)^3}{R^2} = R\left(1 - 3\frac{\Delta R}{R} + \frac{3\Delta R^2}{R^2} - \frac{\Delta R^3}{R^3}\right)$$

and consider solutions of order $\Delta R/R$, where the equations simplify to:

$$\frac{\mathrm{d}R}{\mathrm{d}t} = \frac{g}{3}\left[(r+1)(R - 3\Delta R) - rR\right] \tag{S8}$$

The differential equation is a simple first order linear differential equation and can be solved:

$$R(t) = R_0 \cdot \exp\left(\frac{gt}{3}\right) + 3\Delta R \cdot (r+1) \tag{S9}$$

With R_0 as an integration constant, where the radius at time zero is given from eq. (S9) by $R(0) = R_0 + 3\Delta R \cdot (r+1)$. By going only to order ΔR, we can additionally derive a simplified expression of the critical radius as a function of r and g. As before we set the derivative to zero of eq. (S8) to obtain:

$$(r+1)(R_C - 3\Delta R) - rR_C = 0.$$

Which leads to the solution:

$$R_C = 3(1+r)\Delta R.$$

5.2 Growth rate fitting

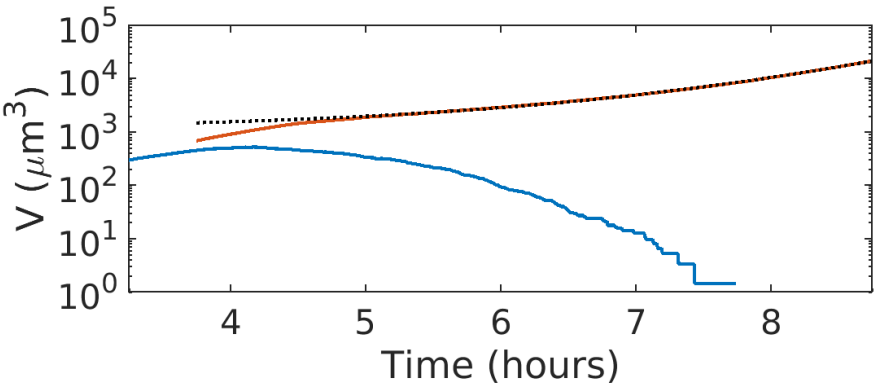

Figure S6: Example of time traces of the colony volume. The blue line is a time-trace from a colony which was just below the survival threshold when the phage attack began. Since the colony is exterminated, a growth rate of zero is assigned. The red line is an example of colony which was just above the survival threshold. The growth rate is determined by fitting of eq. (S9) (black line)

From simulation time-traces, the growth-rate of the colony is fitted to eq. (S9), with R_0 and g being the fitting parameters (Fig. S6 red). When colonies are completely eradicated they are assigned a growth rate of 0 (Fig. S6 blue).

6 Summary of experiments with phage infection of microcolonies at different soft-agar depths

In this section, we summarize the result of two additional repeats of the experiment shown in Fig. 5 in the main text (we call them repeat experiment 1 (exp. 1) and repeat experiment 2 (exp. 2)). The general protocol is given in the Methods section in the main text, with the exception that 3 ml of top agar per plate was used instead of 2.5 ml, and that 250 μl of phage lysate was sprayed onto the plates instead of 500 μl. The phage lysates used in exp. 1 and 2 had concentrations of 4×10^{10} PFU/ml and 3.5×10^{10} PFU/ml, respectively. In addition, in exp. 1, we only prepared one plate for phage spray and one plate for the no-phage control per time point, and the control plates were also used for microscope imaging during the first 8 hours, which means that they were moved from 37°C to room temperature several times during the incubation time.

In both of the repeat experiments, the colony size development was consistent with exponential growth in the first 9 hours, with a fitted doubling time of 29 min and 26 min in exp. 1 and exp. 2, respectively (Fig. S7).

The fraction of visible colonies as a function of pre-incubation time before phage spray is shown in Fig. S8. We see a clear increase in the survival fraction at 6-7 hours, consistent with the result presented in the main text. One notable difference is that in exp. 2, a small number of surviving colonies were observed at all time points, even for the plate sprayed with phage at the 0-hour time point. We noticed, however, that the colonies in the early time-points (especially up to 4 hours) were clustered on one side of the plate, and that the top-agar layer in some cases was noticably thicker on that side of the plate. This suggests that the thicker layer of top-agar provided protection by substantially delaying phage arrival. Therefore, in future experiments, we used the thinnest top agar layer possible (2.5 ml per plate), and care was taken to obtain a homogeneous layer of top agar across the plate.

Finally, Fig. S9 shows the estimate of the radius of final colonies, with and without exposure to phage. The substantial reduction in size as a consequence of phage exposure is seen in both repeat experiments. In exp. 1, the smaller radius from the fluorescence images than from the dark-field images of phage-exposed colonies is evident, suggesting that the surface layer is dead (not producing GFP). In exp. 2, the difference is less pronounced, likely due to additional protection by the thicker top agar.

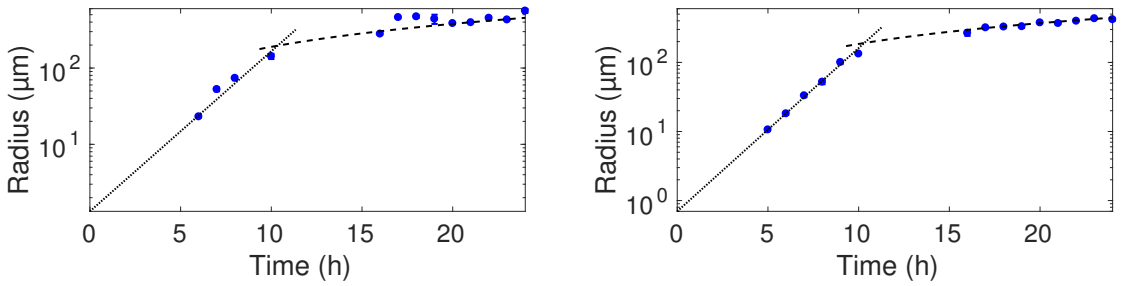

Figure S7: Growth curves for repeat experiment 1 (left) and repeat experiment 2 (right). The fitted doubling time is 28.7 ± 1.2 min and 25.5 ± 0.3 min for exp. 1 and 2, respectively.

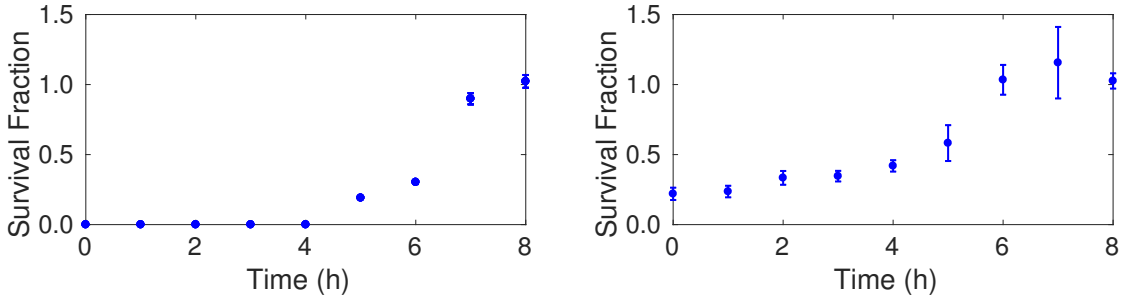

Figure S8: Survival fractions from repeat experiment 1 (left) and repeat experiment 2 (right). The average number of colonies per control plate was 89 ± 4 and 82 ± 4 exp. 1 and 2, respectively.

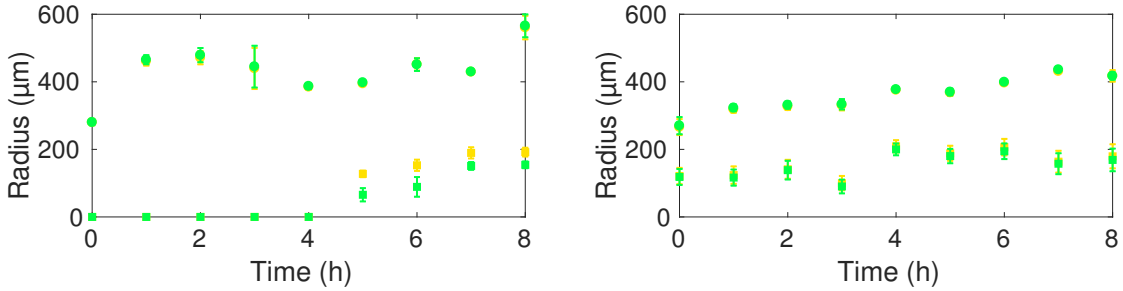

Figure S9: Radii of the final colonies from repeat experiment 1 (left) and repeat experiment 2 (right). The circles show the final colony size in the absence of phage exposure, while the squares show the radii of colonies exposed to phages. The time at which phages were introduced is given on the horizontal axis. Yellow symbols show the radii estimated from dark-field images, while green symbols show the radii estimated from green fluorescence images.

7 Summary of experiments with phage infection of microcolonies with same total growth time

In the experiment shown in Fig. 5, all colonies were incubated for an additional 16 hours following the addition of phages to ensure that the time span allotted for the phages to attack the colonies was uniform across all the plates. As a result, the total incubation time was greater for plates where phages were applied at later time points than for those exposed to phage at early time points. To investigate whether this difference in total incubation time influenced the result, we performed two experiments in which phages were sprayed onto colonies that had been grown for 5, 6 or 7 hours prior to phage exposure, and were then incubated again until they had each reached a total incubation time of 21 hours (set 1) or 23 hours (set 2). We call this repeat experiment 3 (exp. 3). The protocol for exp. 3 was similar to the one described in Methods, with the exception that the phage lysate titer was $\sim 2 \times 10^9$ PFU/ml. For each time point in each set, we had one control plate (no phage added) and one test plate (phage applied at the indicated time point).

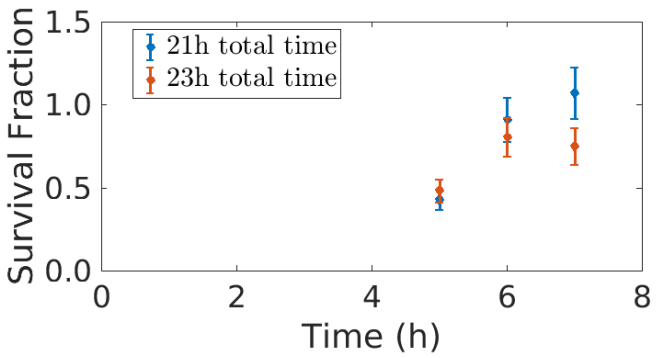

Figure S10: Survival fractions from repeat experiment 3. The average number of colonies per control plate was 19 ± 3. Blue and red data points show the survival fraction of the colonies with 21 or 23 hours of total incubation time, respectively.

Fig. S10 shows the colony survival fraction as a function of incubation time prior to the addition of phage, and Figs. S11 and S12 shows images of several representative colonies from plates sprayed with phages at 5h and 7h, that can be compared to Fig. 4. In conclusion, these experiments confirm that the enhanced survival of colonies sprayed with phages at later time points (shown in Figs. 4 and 5) is not an effect of the longer total incubation time they experienced, but rather an effect of the duration of the incubation time (and therefore colony size) prior to phage addition.

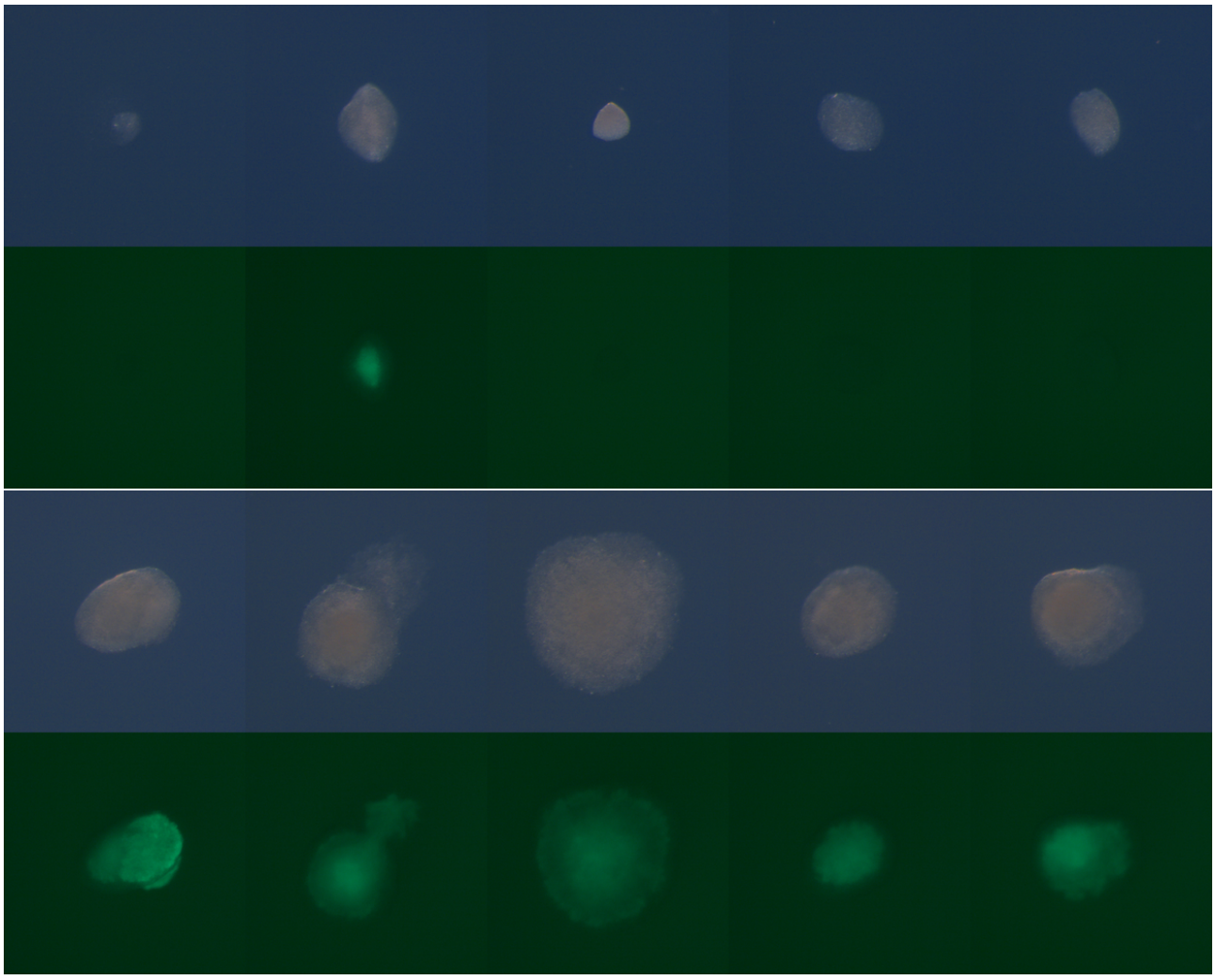

Figure S11: Images of colonies after exposure to phages. These colonies were incubated for 5 hours (top panel) or 7 hours (bottom panel) before being sprayed with phages. The images were captured after additional incubation to reach 21 hours total incubation time.

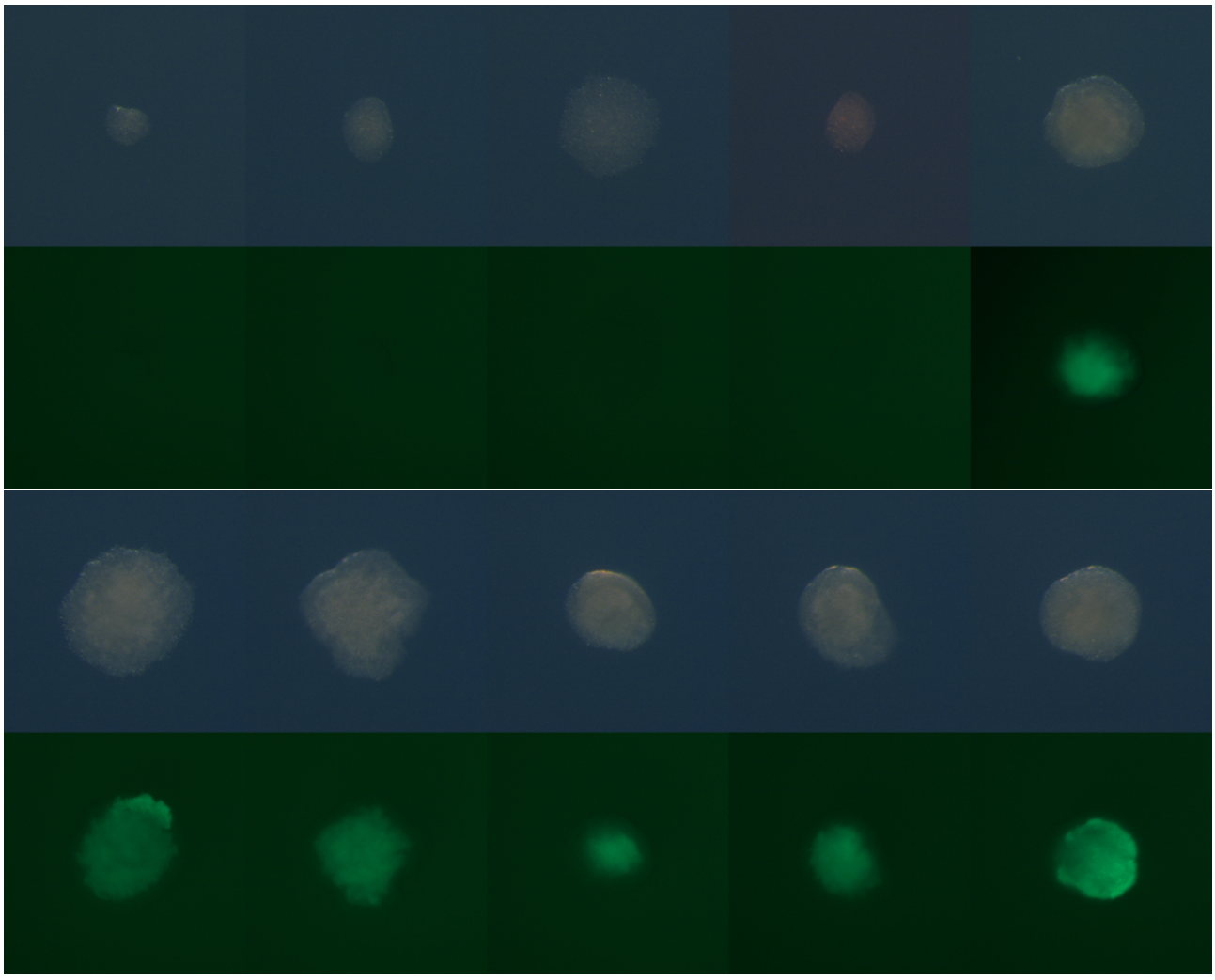

Figure S12: Images of colonies after exposure to phages. These colonies were incubated for 5 hours (top panel) or 7 hours (bottom panel) before being sprayed with phages. The images were captured after additional incubation to reach 23 hours total incubation time.

8 $P1_{vir}$ resistance tests

8.1 Experimental procedures

To determine the level of $P1_{vir}$ resistance among cells in the liquid culture used for seeding the microcolonies, dilutions of the culture in sterile MC buffer were mixed with $P1_{vir}$ at an average phage input >10, incubated for 20 min, and plated on LB plates supplemented with 10 mM MgSO4, 5 mM CaCl2 and 50 μg/ml kanamycin. The frequency of resistant mutants in the culture was calculated as the colony forming units (CFU) per ml of culture treated with phages relative to the CFU per ml of the untreated culture.

To test individual cells in surviving microcolonies from the experiment shown in Fig. 5 for whether they were sensitive or resistant to $P1_{vir}$, 10 individual microcolonies were picked out of the top agar from one plate for each time point of phage application (4-8 hours) and restreaked on individual tryptone plates [5] containing 10 mM sodium citrate to destabilize the phage particles and thereby permit colony formation by both sensitive and resistant cells. 37/50 plates contained *E. coli* colonies after overnight incubation, as shown in Table 1. From these survivors, up to 10 individual colonies were picked from each plate, and cross-streaked against $P1_{vir}$ on R plates (supplemented as in Methods). Since cross-streaks can be difficult to interpret with certainty, any cross-streak where the outcome was unclear was repeated, and, in addition, the outcome of the cross-streak was confirmed for 36 colonies by infection with $P1_{rev6}$ [6] following overnight growth of the colony in shaking liquid culture, and selection for lysogeny on LB plates containing 15 μg/ml chloramphenicol. In every case, the strains that were deemed $P1_{vir}$-sensitive by cross-streak yielded large numbers of chloramphenicol-resistant lysogens, while the strains that were deemed $P1_{vir}$-resistant by cross-streak yielded no or at most a very small number of lysogens, consistent with a small subset of cells having reverted to the P1-sensitive phenotype. Finally, we tested three colonies that were deemed $P1_{vir}$-resistant by cross-streak for their ability to adsorb and propagate $P1_{vir}$ in liquid culture. Specifically, we tested the colonies with id's 5h-3-3, 6h-3-2 and 8h-7-1 from Table S2. At the beginning of the experiment, $P1_{vir}$ were added to diluted liquid cultures containing 1×10^6 CFU/ml to reach an initial phage-to-cell ratio of 0.02. For the following 5.5 hours, the phage content of the mixture was sampled by plaque assay using the double agar overlay method. In the case of the P1-sensitive parent strain SP427, the phage content increased from 3.8×10^4 PFU/ml at the beginning of the experiment to 7.4×10^8 PFU/ml at the last time point. On the contrary, the phage content of the three resistant cultures decreased slightly from $3.8 \times 10^4 \pm 3300$ PFU/ml to $3.0 \times 10^4 \pm 8500$ PFU/ml in the same time span. We conclude that the three tested strains are indeed resistant to infection by $P1_{vir}$, as the phages are unable to propagate on them. They are also refractory to $P1_{vir}$ adsorption, since the number of free phage particles only decreased slightly during the 5.5 hours of growth of the bacterial strains.

8.2 Detailed results of the cross-streak experiment

Table S2 summarizes the detailed results of the $P1_{vir}$ resistance test. As described in the main text, we picked 10 colonies from each phage-sprayed plate that had been pre-incubated for at least 4 hours (shown in the first column), and streaked the colonies on fresh plates containing sodium citrate to inactivate free phage and thereby permit the growth of both sensitive and resistant cells from the original colony. The 10 colonies from each plate are numbered in the second column (Parent colony id #). The third column (# colonies tested) lists the number of "offspring" colonies formed from each parental colony that were tested for phage resistance. When the number is less than 10, it means that less than 10 isolated colonies formed on the fresh plate. When more than 10 colonies grew, we randomly picked 10 for cross-streaking. The fourth column (Resistant), lists the number of colonies that tested $P1_{vir}$ resistant by cross-streaking, while the fifth column (Susceptible) lists the number of colonies that were found to be susceptible to $P1_{vir}$. The sum of the fourth and fifth columns should equal the number in the third column.

Table S2: Full results of the $P1_{vir}$ resistance test.

Time	Parent colony id #	# colonies tested (When less than 10, equal to number of recovered colonies)	Resistant	Susceptible
4h	1	0	-	-
	2	10	3	7
	3	10	0	10
	4	10	0	10
	5	10	0	10
	6	0	-	-
	7	0	-	-
	8	0	-	-
	9	10	10	0
	10	10	0	10
5h	1	0	-	-
	2	1	0	1
	3	10	10	0
	4	0	-	-
	5	0	-	-
	6	0	-	-
	7	0	-	-
	8	10	0	10
	9	1	0	1
	10	10	0	10
6h	1	0	-	-
	2	10	0	10
	3	10	10	0
	4	0	-	-
	5	10	10	0
	6	10	0	10
	7	10	10	0
	8	10	10	0
	9	10	10	0
	10	0	-	-
7h	1	10	10	0
	2	6	5	1
	3	0	-	-
	4	10	10	0
	5	10	0	10
	6	10	0	10
	7	10	0	10
	8	10	10	0
	9	10	10	0
	10	10	0	10
8h	1	10	0	10
	2	10	0	10
	3	10	10	0
	4	10	10	0
	5	10	10	0
	6	10	0	10
	7	10	9	1
	8	10	0	10
	9	10	10	0
	10	10	0	10

9 Effect of the number of phages per bacterium at the time of phage application

In our experimental protocol, we spray the same number of phages onto microcolonies of different sizes, thus the initial average phage input per bacterium (API) decreases for larger microcolony sizes. In order to exclude the possibility that this decrease gives rise to the survival of larger colonies (i.e., protection simply due to a lowered API without any spatial effect), we estimated whether the number of phages applied to the plates would have been sufficient to kill all the phage-sensitive cells had they been in a well-mixed liquid environment rather than a spatially structured environment.

9.1 Host-phage interaction in a well-mixed culture

First, we experimentally measured the change in optical density of bacterial cultures upon exposure to phages at different initial API's in a well-mixed culture. Specifically, 4×10^5 CFU of E. coli SP427 from an overnight culture were subcultured into LB medium supplemented with 10 mM MgSO4, 5 mM CaCl2 and 50 μg/ml kanamycin in each well of a 96-well microtiter plate. Dilutions of $P1_{vir}$ lysate were then added to each well to give the desired API in a total volume of 150 μl. The microtiter plate was incubated at 37°C and shaking at 200 rpm in a Fluostar Omega plate reader, and the optical density of the culture at 600 nm was measured every 5 minutes for 12 hours.

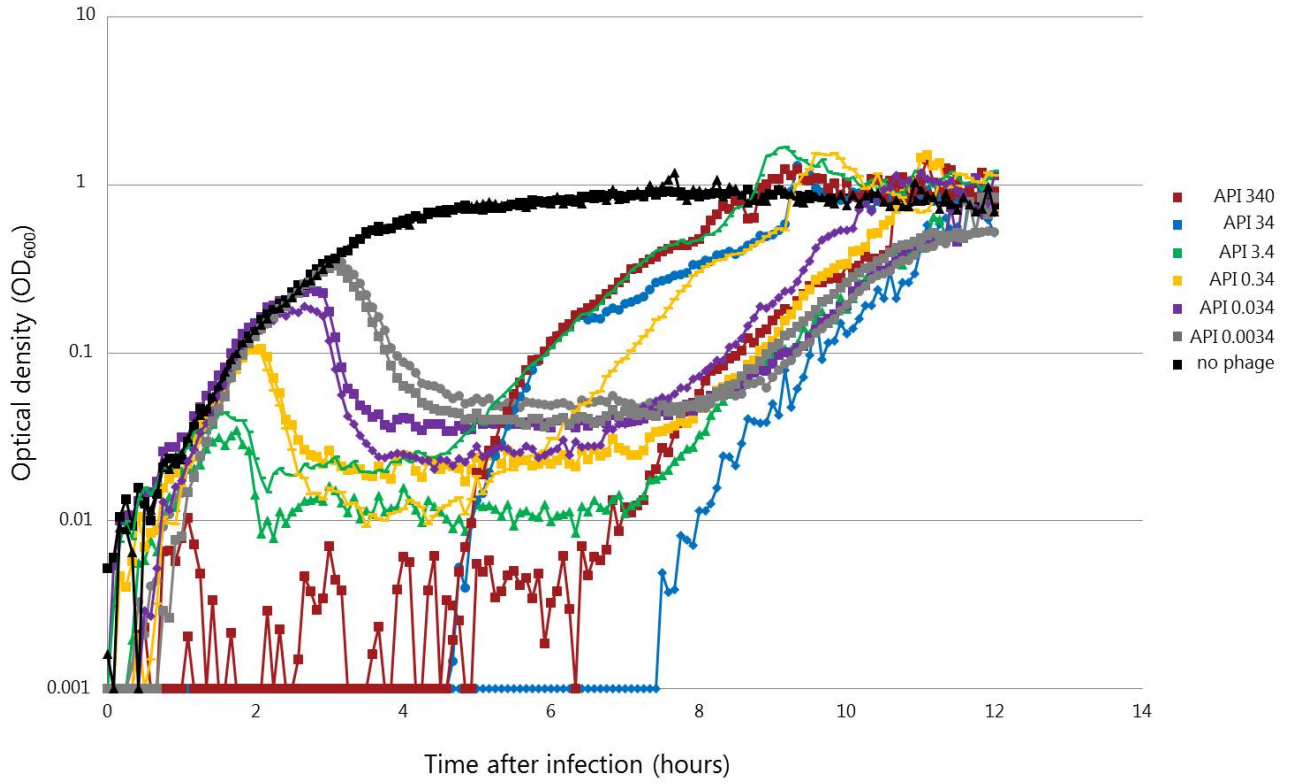

Figure S13: Change of OD_{600} in a well-mixed culture with different initial API's. The values of initial API are displayed in the figure. Two individual measurements are displayed for each value of API. Our measurements of optical density are unreliable at values below 0.01, which explains the large variation in measurements from cultures with very low optical densities.

Fig. S13 shows that for every API, the density of the bacterial population shows a sudden drop after phage addition, but the lag time before the drop occurs increases for smaller API's because the phages need to undergo addtional rounds of multiplication before they are sufficiently numerous to overtake the cell population. Some time after the drop, the OD_{600} increases again and finally plateaues at a similar level as the control cultures where no phage were added (black lines). The second increase is due to the presence of phage-resistant mutants which eventually accumulate. The time at which the resistant mutants accumulate varies between duplicate cultures containing the same initial API, reflecting the stochastic nature of the appearance of resistant mutants [7]. For every tested API, a significant reduction of the host population was observed within 4 hours. From 1h to 4h, the OD_{600} for the no-phage control culture increased about 20-30 fold, corresponding to 4-5 doublings. It is difficult to evaluate the OD_{600} in the first 1h, but evaluating from the later growth rate, at most 1-2 doublings

occurred during that period. This shows that about 6 doubling times after phage encounter gave sufficient time for the phages to kill the hosts even at the low initial API's.

9.2 Evaluation of initial API in the microcolony experiments

We now evaluate whether the amount of phages applied to the plates in the spatially structured microcolony experiment would be enough to eliminate the sensitive hosts had they been in a well-mixed culture. We consider the time point where phages were applied after 7 hours of incubation, at which time all of the colonies survived in the experiment shown in Figs. 4 and 5.

The initial API in our experiment is not straightforward to estimate because of the spatial structure, so we have made two different estimates.

The simplest evaluation of the API is to consider the ratio: (total number of phages sprayed per plate)/(total number of cells per plate). We sprayed 3.5×10^9 phages per plate, and the plates with 7 hours of incubation have about 76 colonies of 10^5 cells per colony. The resulting API$\sim 4.6 \times 10^2$ would certainly be high enough to almost immediately clear the sensitive host population (compare to Fig. S13 at API 340).

However, in reality, many of the applied phages may not have encountered a colony. To take this into account, we now assume that the phages are sprayed uniformly across the surface of the plate ($\sim$ 9 cm in diameter), and we make the very conservative assumption that the colony is only attacked by the phages that land directly on top of it (so that the cross-section of the colony from the top view determines the number of phages that hit it, and the phages do not arrive at the colony by diffusion in the horizontal plane). In this case, the number of phages per colony for the 7h incubation time is estimated to be $\sim 1.5 \times 10^3$, resulting in a lower bound on the initial API of ~ 0.01, which falls within the tested range in Fig. S13 that would have resulted in killing of the phage-sensitive cells after a lag time of less than 6 doubling times. We know that the 7h colonies had nutrients left to support more than 6 doublings after phage exposure, because in the experiment shown in Figs. 4 and 5, the 7h colonies of 30 μm radius had grown to 350 μm in radius in the absence of phages by the end of the experiment, so the volume had increased more than 1000 fold, meaning that the nutrients available after 7 hours supported about 10 additional doublings of the population. Thus, there would have been ample time for the phages to eliminate all the phage-sensitive cells had they been growing in a well-mixed culture. Therefore, we conclude that the reduction of the initial API at increasing microcolony size is not the main determinant of the survival threshold.

References

[1] N. Mitarai, M. H. Jensen, and S. Semsey, "Coupled positive and negative feedbacks produce diverse gene expression patterns in colonies," *Mbio*, vol. 6, no. 2, pp. e00059–15, 2015.

[2] H. Cho, H. Jnsson, K. Campbell, P. Melke, J. W. Williams, B. Jedynak, A. M. Stevens, A. Groisman, and A. Levchenko, "Self-organization in high-density bacterial colonies: Efficient crowd control," *PLOS Biology*, vol. 5, pp. 1–10, 10 2007.

[3] N. Mitarai, S. Brown, and K. Sneppen, "Population dynamics of phage and bacteria in spatially structured habitats using phage λ and escherichia coli," *Journal of bacteriology*, vol. 198, no. 12, pp. 1783–1793, 2016.

[4] M. De Paepe and F. Taddei, "Viruses' life history: towards a mechanistic basis of a trade-off between survival and reproduction among phages," *PLoS Biol*, vol. 4, no. 7, p. e193, 2006.

[5] J. H. Miller, *Experiments in Molecular Genetics*. Cold Spring Harbor, New York: Cold Spring Harbor Lab., 1982.

[6] N. L. Sternberg and R. Maurer, "[2] bacteriophage-mediated generalized transduction in escherichia coli and salmonella typhimurium," *Methods in enzymology*, vol. 204, pp. 18–43, 1991.

[7] S. E. Luria and M. Delbrück, "Mutations of bacteria from virus sensitivity to virus resistance," *Genetics*, vol. 28, no. 6, p. 491, 1943.